OPEN ACCESS Freely available online

PLoS GENETICS

Bub1-Mediated Adaptation of the Spindle Checkpoint

Greicy H. Goto[1], Ashutosh Mishra[2], Rashid Abdulle[1], Clive A. Slaughter[2], Katsumi Kitagawa[1]*

1 Center for Childhood Cancer, The Research Institute at Nationwide Children's Hospital, Columbus, Ohio, United States of America, **2** Hartwell Center for Bioinformatics and Biotechnology, St. Jude Children's Research Hospital, Memphis, Tennessee, United States of America

Abstract

During cell division, the spindle checkpoint ensures accurate chromosome segregation by monitoring the kinetochore–microtubule interaction and delaying the onset of anaphase until each pair of sister chromosomes is properly attached to microtubules. The spindle checkpoint is deactivated as chromosomes start moving toward the spindles in anaphase, but the mechanisms by which this deactivation and adaptation to prolonged mitotic arrest occur remain obscure. Our results strongly suggest that Cdc28-mediated phosphorylation of Bub1 at T566 plays an important role for the degradation of Bub1 in anaphase, and the phosphorylation is required for adaptation of the spindle checkpoint to prolonged mitotic arrest.

Citation: Goto GH, Mishra A, Abdulle R, Slaughter CA, Kitagawa K (2011) Bub1-Mediated Adaptation of the Spindle Checkpoint. PLoS Genet 7(1): e1001282. doi:10.1371/journal.pgen.1001282

Editor: Sue Biggins, Fred Hutchinson Cancer Research Center, United States of America

Received December 31, 2009; **Accepted** December 20, 2010; **Published** January 27, 2011

Funding: This work was supported by NIH grant GM68418 and by American Cancer Society Research Grant RSG-07-144-01-CCG. The funders had no role in study design, data collection and analysis, decision to publish, or preparation of the manuscript.

Competing Interests: The authors have declared that no competing interests exist.

* E-mail: Katsumi.Kitagawa@nationwidechildrens.org

Introduction

The kinetochore, composed of centromere DNA and associated proteins, mediates the attachment of chromosomes to spindle microtubules and directs chromosome movement during mitosis and meiosis, thus maintaining the high fidelity of chromosome transmission during cell division. The plus ends of microtubules are captured and stabilized by kinetochores, causing chromosomes to mono-orient to 1 pole [1–3]. Replicated chromosomes are composed of 2 chromatids, each with its own kinetochore. Chromosomes become bi-oriented when sister kinetochores are captured by a microtubule emanating from the opposite pole [4–7]. Sister chromatids remain paired until all chromosomes achieve correct bi-orientation. Sister chromatid cohesion is regulated by the control of separase activity [2,8–11]. Sister chromatids disjoin after all chromosomes are bi-oriented, marking the onset of anaphase; this lack of cohesion allows each chromatid to move to its respective pole. The metaphase-to-anaphase transition and exit from mitosis are initiated by a ubiquitin-mediated proteolysis complex called the cyclosome or anaphase-promoting complex (APC/C). Before anaphase, separase is inactive because it is bound to securin [9]. Anaphase is initiated by the ubiquitin-mediated proteolysis of securin, which is triggered by activation of the APC/C^{Cdc20} [12].

The spindle checkpoint regulates faithful chromosome segregation during mitosis by monitoring the bipolar kinetochore–microtubule interaction and delaying the onset of anaphase until stable bipolar attachment is achieved [13]. Genes involved in the spindle checkpoint were first isolated from *Saccharomyces cerevisiae* and include *MAD1*, *MAD2*, and *MAD3* (mitotic arrest–deficient); [14] *BUB1* and *BUB3* (budding uninhibited by benzimidazoles [a microtubule-depolymerizing drugs]) [15]; and *MPS1* (monopolar spindle) [16]. Mutual inhibition between the APC/C and Mps1, an essential component of the spindle checkpoint, causes sustained inactivation of the spindle checkpoint that cannot be reactivated in anaphase [17], and two groups have recently reported that protein phosphatase 1 activity is required for silencing the spindle checkpoint by reversing key phosphorylation events [18,19].

The duration of mitotic arrest induced by the spindle checkpoint is not indefinite [20,21]. Thus, cells eventually exit from mitosis and re-enter interphase. Because continued activation of the spindle checkpoint is lethal, adaptation to the spindle checkpoint arrest is beneficial so that cells have a chance to survive rather than undergo certain death [13,22]. However, the mechanism of adaptation that could occur by spindle checkpoint inactivation remains to be characterized.

We report here that Cdc28-mediated phosphorylation of T566 plays an important role in Bub1 degradation in anaphase, and this phosphorylation is essential for deactivating the spindle checkpoint in anaphase and adaptation to prolonged mitotic arrest.

Results

Bub1 is phosphorylated at threonine-566 in a Cdc28-dependent manner *in vivo*

To study whether phosphorylation of Bub1 contributes to its degradation, we determined the phosphorylation sites of Bub1 by mass spectrometry. From extracts of cells expressing myc-tagged Bub1, myc-tagged Bub1 was immunoprecipitated with anti-myc antibody conjugated to Sepharose. Mass spectrometry of immunoprecipitated myc-tagged Bub1 revealed that threonine-566 (T566) on Bub1 is phosphorylated (Figure 1A).

To monitor the status of T566 phosphorylation, we generated polyclonal antibodies against an oligopeptide containing phosphorylated T566. Antibody specificity for T566 phosphorylation was verified by immunoprecipitating myc-tagged Bub1 and Bub1-T566A followed by phosphatase treatment of immunoprecipitates (Figure 1B). The band that is recognized by the phospho-T566 antibodies in wild-type cells is absent upon phosphatase treatment, confirming the specificity of phospho-T566 antibodies for phosphorylated Bub1 (Figure 1B).

Author Summary

The spindle checkpoint protects cells from aneuploidy by monitoring the status of the kinetochore-microtubule attachment. Defects in this checkpoint pathway and in kinetochore-microtubule attachment can cause substantial aneuploidy in cells. The duration of the mitotic arrest induced by the spindle checkpoint is not indefinite: cells eventually exit from mitosis and re-enter interphase. Because continued activation of the spindle checkpoint is lethal, adaptation to the spindle checkpoint arrest is essential so that cells have a chance for survival as opposed to certain death. However, adaptation of the spindle checkpoint has a flip side—adapted cells could have an increased chance of aneuploidy due to premature mitotic exit. Thus, it is essential that this mechanism be regulated appropriately. Despite the importance of understanding the adaptation of the spindle checkpoint, little is known to date about this mechanism. We found that Cdc28-mediated phosphorylation of Bub1 at T566 plays an important role for adaptation of the spindle checkpoint, a finding providing the molecular insight on how adaptation to prolonged mitotic arrest induced by the spindle checkpoint occurs.

We used the phospho-T566 antibodies to identify the kinase responsible for T566 phosphorylation. Sequence analysis revealed that T566 is within a potential phosphorylation site for the Cdk1/Cdc28 kinase [23]. To determine whether Cdc28 is required for T566 phosphorylation of Bub1, we analyzed wild-type strains and *cdc28-1N* mutants arrested in metaphase by nocodazole treatment and incubated at the nonpermissive temperature of 37°C. Phosphorylated T566 was abolished in *cdc28-1N* mutant cells, indicating that Cdc28 is required for T566 phosphorylation on Bub1 *in vivo* (Figure 1C). We also found that this phosphorylation is independent of the kinase activity of Bub1 (Figure S1). In addition, as Bub1 and Mps1 kinases act together at an early step in the spindle checkpoint pathway [24] and as Mps1 is a serine/threonine kinase [24], we also examined whether Mps1 is required for T566 phosphorylation of Bub1. However, phosphorylated T566 was not abolished in *mps1-1* mutant cells at the nonpermissive temperature of 37°C, suggesting that Mps1 is not required for T566 phosphorylation on Bub1 *in vivo* (Figure S2).

Immunoprecipitated Cdc28 was able to efficiently phosphorylate the maltose binding protein (MBP)-fused Bub1 fragment (400–700 amino acids) but not MBP-Bub1 with T566A (400–700 amino acids), indicating that Cdc28 phosphorylates T566 on Bub1 *in vitro* (Figure 1D).

T566 phosphorylation plays a role in adaptation of the spindle checkpoint

Next, we examined the *in vivo* function of T566 phosphorylation. *BUB1-T566A* (this mutant is dominant, Figure S3) and *bub1Δ* mutant cells were sensitive to the microtubule-depolymerizing drug nocodazole (at 2.5 μg/mL and 10 μg/mL) or benomyl on a plate (Figure 2A and data not shown), suggesting that T566 phosphorylation is important for spindle checkpoint function. Thus, we examined whether *BUB1-T566A* mutant cells can be arrested in metaphase with nocodazole. Interestingly, a FACS analysis showed that *BUB1-T566A* mutant cells, but not *bub1Δ* mutant cells, were arrested in G2/M by nocodazole treatment (Figure 2B and Figure S4). Therefore, *BUB1-T566A* mutant cells can activate the spindle checkpoint in response to microtubule depolymerization.

Interestingly, FACS analysis showed that wild-type cells appeared to be "adapted" to nocodazole at a high concentration (10 μg/mL; nocodazole is nearly saturated at 10 μg/mL in water) [25] after incubation at 30°C for 5 h but *BUB1-T566A* mutant cells were still tightly arrested in G2/M (Figure 2B). Analysis of nuclear morphology over time revealed that adaptation to the mitotic arrest results in G1 cells (unbudded or small budded – types 1 and 2) rather than in rebudded cells without cell division (Figure 2C and 2D – type 6) and that half of these G1 cells did not have nuclei (Figure 2C and 2D – type 1), suggesting that premature cytokinesis occurred without chromosome segregation (Figure 2C and 2D). Consistent with these results, Clb2 levels started to decrease after incubation for 3 h in wild-type cells but not in *BUB1-T566A* mutant cells (Figure 2E). These results indicate that *BUB1-T566A* mutant cells were arrested in mitosis longer than wild-type cells in the presence of nocodazole at the high concentration.

We also studied the adaptation status of cells at a low concentration of nocodazole (2.5 μg/mL). At this concentration, normal cytokinesis probably occurs because the microtubules are not completely depolymerized. FACS analysis and a count of adapted cells over time suggest that there is a substantial delay in adaptation in *BUB1-T566A* mutant cells (Figure 3A and 3B). Time-lapse analyses revealed that *BUB1-T566A* mutant cells stayed longer (~12 h) in mitosis in the presence of nocodazole at a low concentration (Figure 3C, Video S1 and S2). These results strongly suggest that *BUB1-T566A* mutant cells fail to adapt to the spindle checkpoint activated by nocodazole treatment after a prolonged mitotic arrest.

However, it is possible that *BUB1-T566A* mutant cells are sensitive to nocodazole on a plate because metaphase-arrested mutant cells cannot recover from mitotic arrest (i.e., microtubules cannot reassemble on kinetochores). To test this possibility, cells were arrested by nocodazole treatment, nocodazole was washed away, and then budded cells were counted. The increase in the number of budded *BUB1-T566A* mutant cells after the release was comparable to that of wild-type cells (Figure 4A), indicating that *BUB1-T566A* mutant cells can recover from nocodazole-induced mitotic arrest. Furthermore, in a viability assay after nocodazole incubation for several hours, *BUB1-T566A* mutant cells were more viable than *bub1Δ* mutant cells and as viable as wild-type cells (Figure 4B and Figure S5).

Therefore, we conclude that *BUB1-T566A* mutant cells do not grow on a nocodazole/benomyl plate because they are arrested in mitosis for a prolonged period as they cannot "adapt" and not because they die due to premature mitotic exit as in the case of *bub1Δ* mutant cells.

T566 phosphorylation affects Bub1 stability in mitosis

To examine the effect of phosphorylation of T566 on Bub1 stability, the HA-tagged nonphosphorylated mutant protein (T566A) was expressed from the *GAL1* promoter and expression was induced for 2 h before terminating transcription by adding glucose. Indeed, the Bub1-T566A mutant protein was more stable than the wild-type protein in anaphase but not in G1 (Figure 4C and Figure S6), indicating that T566 phosphorylation is important for Bub1 degradation in anaphase.

In addition, we monitored the protein levels of myc-tagged Bub1 and Bub1-T566A mutant proteins expressed from the endogenous promoter in the presence of nocodazole at 30°C over time. FACS profiles obtained under the same conditions showed that adaptation seemed to start around 3 h after addition of nocodazole (Figure 2B).

Consistently, Bub1 protein reduced significantly after 3 h of incubation with nocodazole (Figure 4D, left and Figure S7), whereas the Bub1-T566A mutant protein appeared to be more stable for 5 h incubation with nocodazole (Figure 4D, right and Figure S7).

T566A mutation does not affect kinase activity and chromosome segregation function of Bub1

Fernius and Hardwick showed that the Bub1 kinase domain is required for accurate chromosome bi-orientation after nocodazole

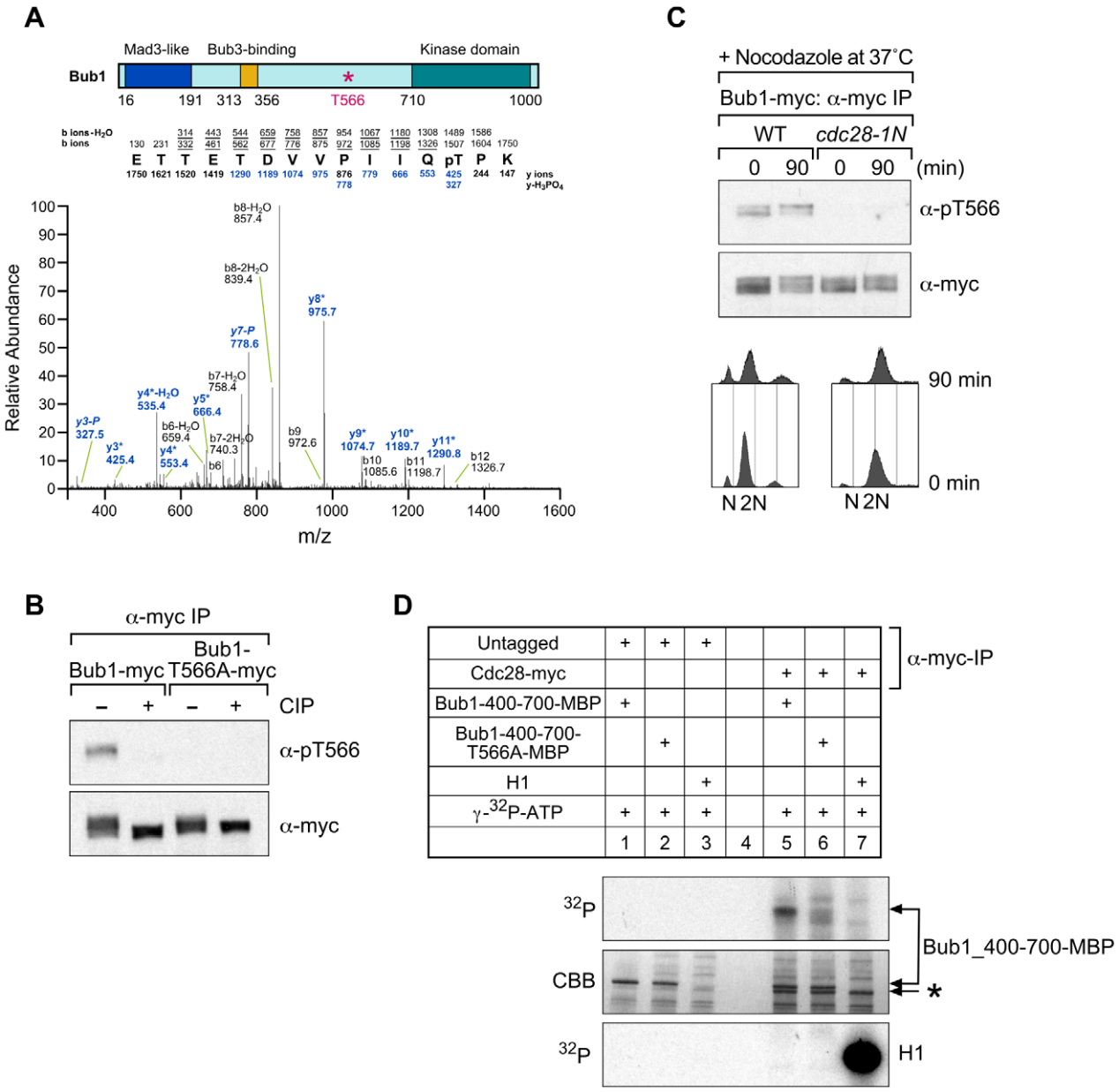

Figure 1. Threonine 566 on Bub1 is phosphorylated dependently on Cdc28 *in vivo*. (A) Cycling cells with Bub1-myc were lysed and immunoprecipitated with antibody to the myc epitope. Immunoprecipitates were digested with trypsin and analyzed by mass spectrometry. The coverage of the identified peptides was 23%. The phosphorylation site was confirmed as threonine 566 (T566) on the basis of the MS/MS data. The phosphorylated peptide sequence and characteristic ions representing loss of phosphoric acid ($-H_3PO_4$) are shown. (B) Antiphosphorylated T566 antibodies. Strains with Bub1-myc or Bub1-T566A-myc were lysed and immunoprecipitated with antibody to the myc epitope. Immunoprecipitates were incubated with and without calf intestinal phosphatase (CIP) and analyzed with anti-phospho-T566 antibody (α-pT566). The membrane was then stripped and immunoblotted with antibody to the myc epitope (α-myc). (C) Phosphorylation of T566 on Bub1 requires Cdc28. Wild-type and *cdc28-1N* cells with Bub1-myc were grown at 25°C and then shifted to 37°C for 90 min in the presence of nocodazole (15 μg/mL). Cells were lysed and immunoprecipitated with antibody to the myc epitope. Immunoprecipitates were analyzed with anti-phospho-T566 antibody (α-pT566). The membrane was then stripped and immunoblotted with antibody to the myc epitope (α-myc). DNA content was measured by FACS analysis. (D) Cdc28 phosphorylates T566 on Bub1 *in vitro*. Wild-type cells with and without myc-tagged Cdc28 were incubated with nocodazole (15 μg/mL) at 30°C for 90 min. Cells were lysed and immunoprecipitated with antibody to the myc epitope. Immunoprecipitates were incubated with 100 μM ATP, 0.2 μCi [gamma-^{32}P]ATP with and without histone H1, MBP fused recombinant protein Bub1_400-700-MBP (MBP-fused Bub1 fragment 400–700 amino acids), and Bub1_400-700-T566A-MBP (MBP-fused Bub1 fragment 400–700 amino acids with T566A change). Coomassie Brilliant Blue staining (CBB) is shown as a loading control. A background band is indicated by the asterisk (*).
doi:10.1371/journal.pgen.1001282.g001

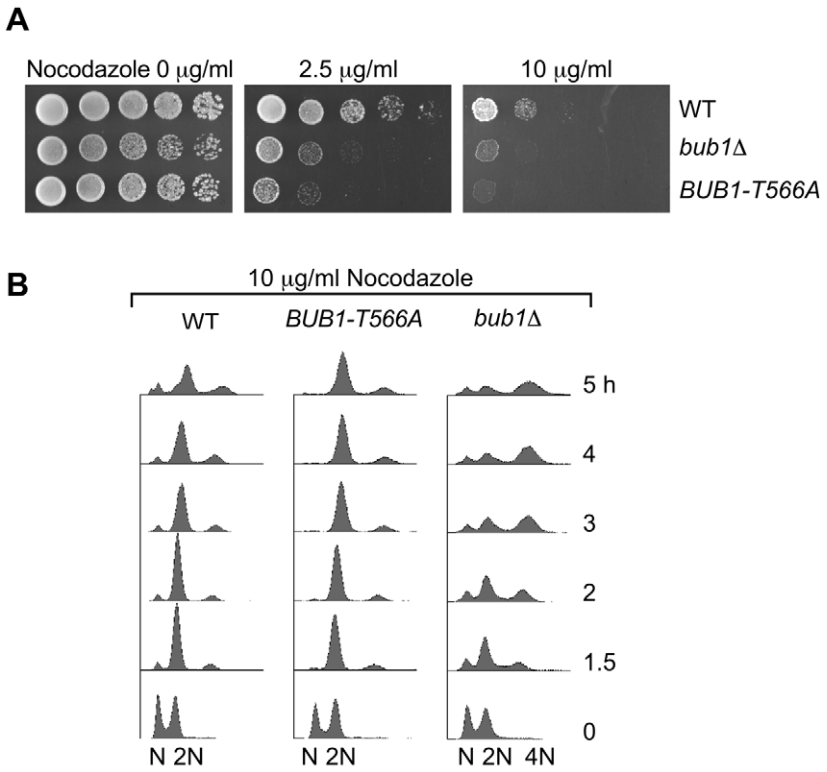

C

								others
WT		**1**	**2**	**3**	**4**	**5**	**6**	**7**
1.5h	n=108	2.8%	1.9%	72.2%	22.2%	0.9%	0%	0%
2h	n=142	5.5%	4.8%	68.2%	16.1%	4.8%	0.6%	0%
3h	n=133	5.3%	0.8%	73.6%	12.7%	6%	0.8%	0.8%
4h	n=134	10.4%	10.4%	62%	12%	3%	1.5%	0.7%
5h	n=148	7.4%	10.8%	54%	17.6%	5.4%	2.8%	2%
BUB1-T566A								
1.5h	n=172	4.6%	2.3%	56%	22%	14%	1.1%	0%
2h	n=133	3%	3%	50.4%	29.3%	11.3%	3%	0%
3h	n=116	3.5%	1.7%	57.8%	14.7%	20.7%	0.8%	0.8%
4h	n=136	5.1%	2.2%	40.4%	22.8%	26.5%	1.5%	1.5%
5h	n=109	4.6%	2.8%	42.2%	28.4%	14.7%	5.5%	1.8%

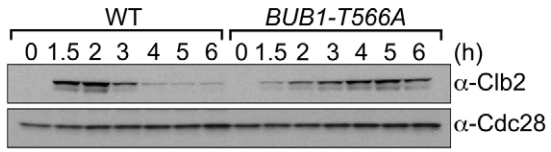

Figure 2. *BUB1-T566A* mutant cells are deficient in adapting to mitotic arrest induced by nocodazole treatment. (A) *BUB1-T566A* mutant cells were sensitive to nocodazole on a plate. Wild-type (WT), *BUB1-T566A*, and *bub1Δ* mutant cells were spotted in 5-fold dilutions from 4×10^7 cells per spot on YPD plates containing nocodazole (2.5 and 10 μg/mL). (B) Wild-type (WT), *bub1Δ*, and *BUB1-T566A* cells were incubated with nocodazole (10 μg/mL) for 1.5, 2, 3, 4 and 5 h; at the indicated times, samples were taken for FACS analysis. (C) Cell and nuclear morphologies. Wild-type (WT) and *BUB1-T566A* cells were incubated with nocodazole (10 μg/mL) for 1.5, 2, 3, 4 and 5 h; at the indicated times, samples were fixed with 4% paraformaldehyde and stained with DAPI. Percentages of indicated morphologies are presented. (D) Representative pictures of cell and nuclear morphologies analyzed in Figure 2C. 1: an unbudded cell without a nucleus, 2: an unbudded cell with a nucleus, 3: a large budded cell with a nucleus in the mother cell, 4: a large budded cell with a nucleus at the neck in the mother cell, 5: a large budded cell with a nucleus at the neck between the mother cell and the daughter cell, and 6: a rebudded cell with a nucleus. Bar, 5 μm. (E) Clb2 levels in nocodazole-treated cells. Wild-type (WT) and *BUB1-T566A* cells were incubated with nocodazole (10 μg/mL) for 1.5, 2, 3, 4, 5 and 6 h; at the indicated times, samples were taken for Western blot analyses with Clb2 antibody. Cdc28 was used as a loading control.
doi:10.1371/journal.pgen.1001282.g002

treatment and that cells lacking the kinase domain are sensitive to microtubule drugs despite being able to arrest in response to kinetochore–microtubule attachment defects [26]. They concluded this because the kinase deletion mutants display significant chromosome missegregation when released from nocodazole arrest [26]. Therefore, we examined whether the *T566A* mutation affects Bub1 kinase activity and chromosome segregation function.

Immunoprecipitated myc-tagged wild-type Bub1 and Bub1-T566A proteins were used for the *in vitro* kinase assay, and both proteins phosphorylated histone H2A and H3 comparably (Figure 5A and Figure S8), indicating that *T566A* mutation does not affect kinase activity.

More importantly, *BUB1-T566A* mutant cells do not show a significant chromosome missegregation phenotype in colony-

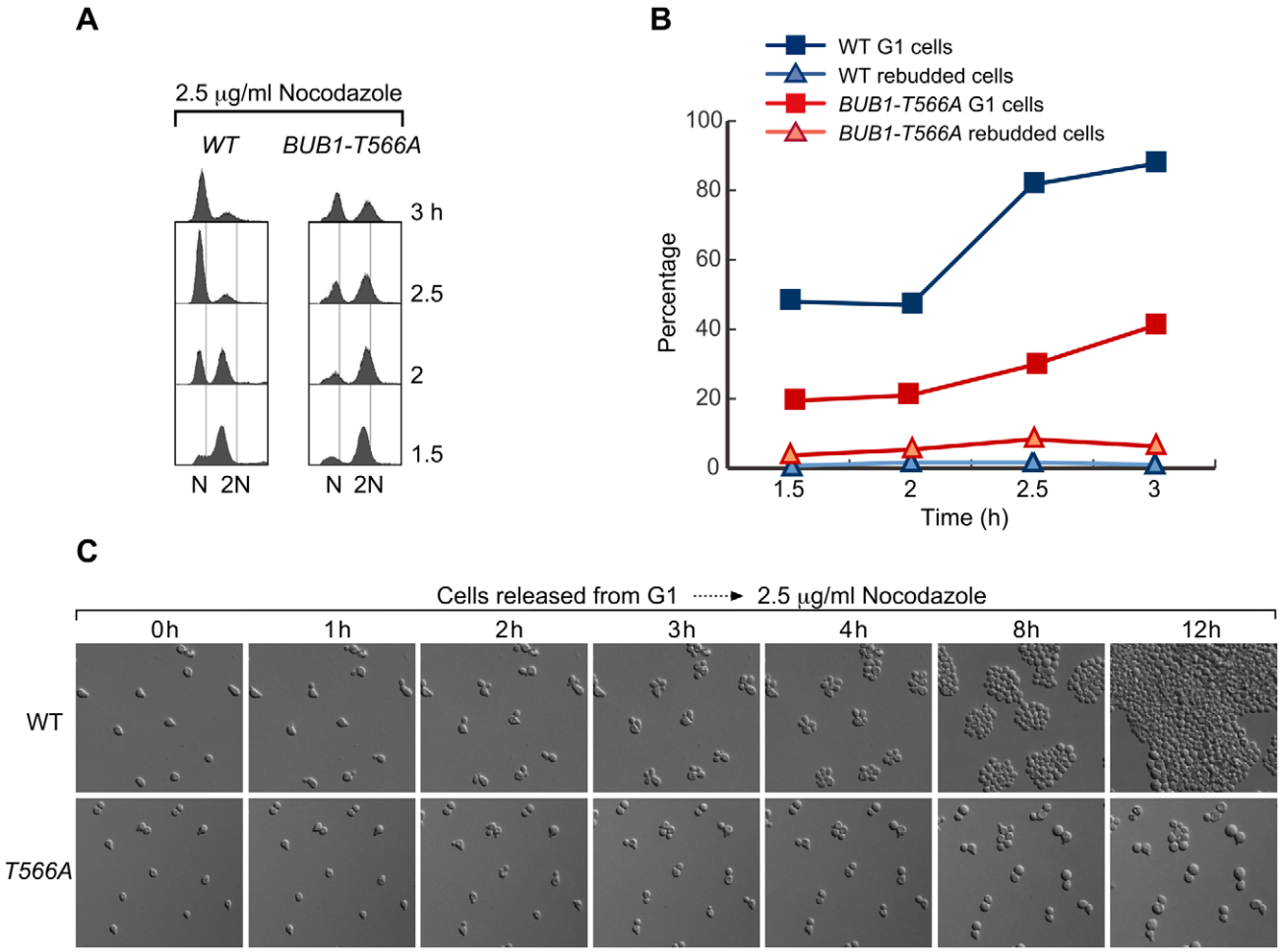

Figure 3. *BUB1-T566A* mutant cells are deficient in adapting to mitotic arrest induced by nocodazole at a low concentration. (A) Wild-type (WT) and *BUB1-T566A* cells were arrested using alpha-factor and released into medium containing 2.5 μg/mL nocodazole at 30°C. After 1 h, alpha-factor was added to the medium and samples were taken for FACS analysis at the indicated times. (B) Graph representing the G1 and rebudded cells shown in Figure 3A. The percentages of G1 and rebudded cells were scored in samples taken at the indicated times (n = 100). (C) Wild-type (Video S1) and *BUB1-T566A* (Video S2) mutant cells were arrested by alpha-factor and released from G1 onto plates containing 2.5 μg/mL nocodazole at 30°C. Time-lapse images of representative examples of each strain were taken at the indicated times.
doi:10.1371/journal.pgen.1001282.g003

sectoring assays [27,28] (Figure 5B), in diploid bimater assay (Figure 5C) [29] or in a faker assay (Figure 5D) [29]. These results indicate that *T566A* mutation does not affect the chromosome segregation function of Bub1. Therefore, there is no kinetochore defect that can activate the spindle checkpoint in *BUB1-T566A* mutant cells.

These results suggest that the stability change caused by the *T566A* mutation contributes to the lack-of-adaptation phenotype of *BUB1-T566A* mutant cells.

Discussion

We have shown that in yeast, Cdc28-mediated T566 phosphorylation of Bub1 facilitates Bub1 degradation in anaphase and thus deactivation of the spindle checkpoint in anaphase. This phosphorylation is required to adapt to prolonged mitotic arrest.

Inactivation of the spindle checkpoint in a normal cell cycle

Mps1 protein abundance decreases in anaphase and Mps1 is a target of the APC/C [17], which is a mechanism of inactivating the spindle checkpoint in anaphase. The 3-D boxes on yeast Mps1 are required for its degradation in anaphase [17], and the KEN-box on human Bub1 is required for its degradation by APC/C in mitosis [30]. However, the D-boxes or KEN-box on Bub1 are not involved in its degradation during anaphase (will be described elsewhere). T566 phosphorylation of Bub1 is important for its degradation at least in part in anaphase. Similar to findings from previous studies that levels of human Bub1 peak in mitosis and are low in G1/S phase [30,31], we found that in the budding yeast Bub1 levels peak in G2/M and drop in late anaphase or G1 (Figure S9 and S10) as described previously [32]. Consistent with this, T566 phosphorylation peaks in G2/M (Figure S9 and S10). However, T566 phosphorylation is not essential to exit from mitosis, suggesting another mechanism to degrade Bub1. Indeed, we found that another site (amino acids 301-400) is important for Bub1 degradation in anaphase (will be described elsewhere). Also, we have not directly demonstrated that degradation of Bub1 caused by T566 phosphorylation is required for adaptation. There is a possibility that T566 phosphorylation is required for adaptation by unknown mechanisms. Further analysis is required to clarify these issues.

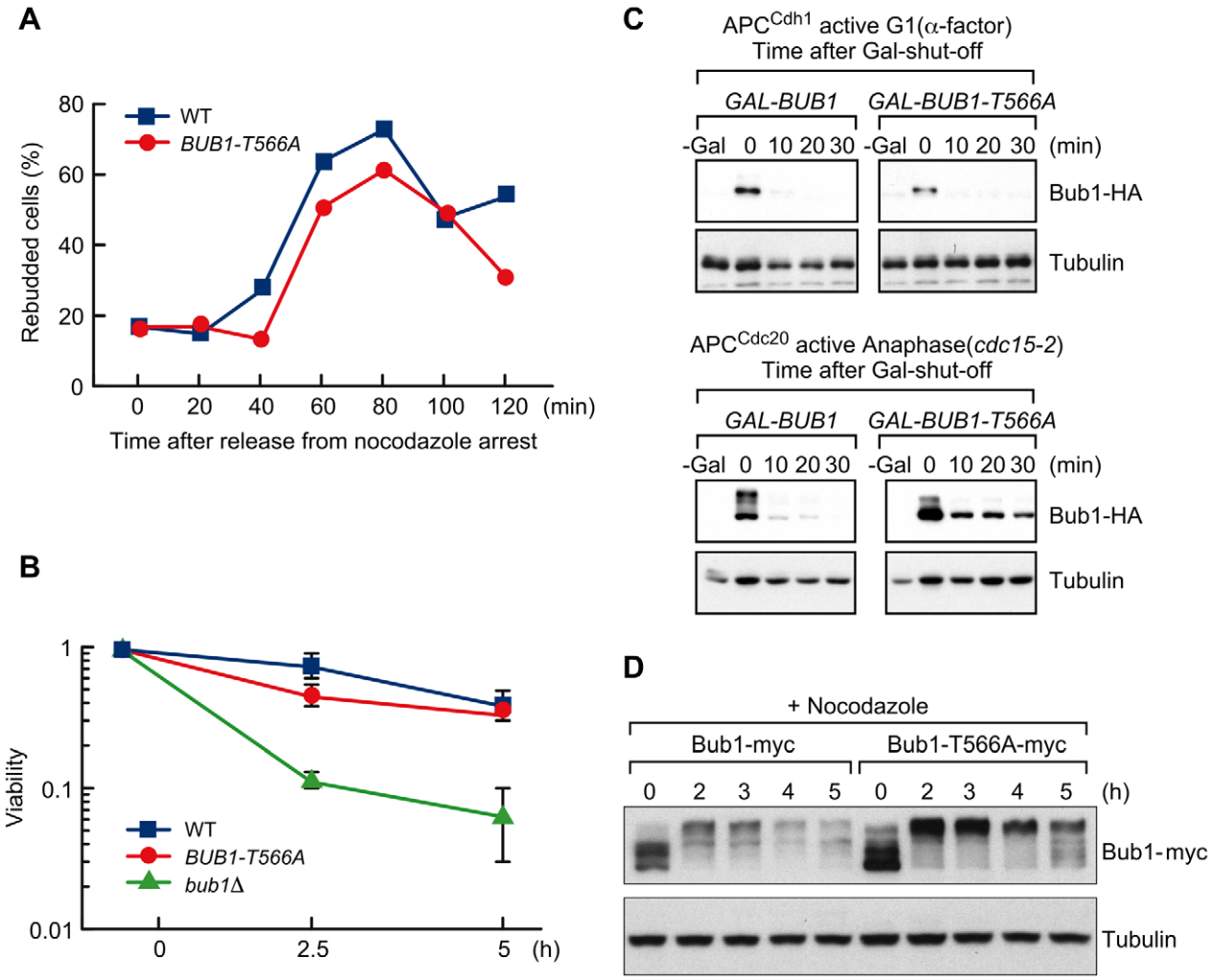

Figure 4. T566 phosphorylation affects Bub1 stability. (A) *BUB1-T566A* mutant cells do not show substantial delay in recovering from nocodazole arrest. Wild-type (WT) and *BUB1-T566A* mutant cells were incubated with nocodazole (15 μg/mL) at 30°C for 90 min and then released from nocodazole arrest; at the indicated times, samples were taken to measure rebudded cells. (B) *BUB1-T566A* mutant cells show no significant sensitivity to nocodazole in a survival assay. Wild-type (WT), *bub1Δ*, and *BUB1-T566A* cells were incubated with nocodazole (15 μg/mL); at the indicated times, cells were washed out and approximately 200 cells were plated on a YPD plate. Cell viability was calculated by dividing the number of colonies formed at the 2.5 and 5 h time points by that formed in the absence of nocodazole (0 h) at 30°C. (C) Phosphorylation of T566 is important for degradation of Bub1 during anaphase but not during G1. *cdc15-2* cells with HA-tagged Bub1 or Bub1-T566A expressed by the *GAL1* promoter (*GAL-BUB1* and *GAL-BUB1-T566A*) were arrested in anaphase (*cdc15-2*) or in G1 (alpha-factor) and then transferred to medium containing galactose for 2 h to induce Bub1 expression. Glucose was added to shut-off Bub1 expression; samples were taken at the indicated times for Western blot analyses with antibody to the HA epitope. Tubulin was used as a loading control. (D) The Bub1-T566A protein is more stable than wild-type in the presence of nocodazole. Wild-type and *BUB1-T566A* mutant cells (Bub1 and Bub1-T566A are tagged with myc) were incubated in the presence of nocodazole (10 μg/mL) at 30°C; at the indicated times, samples were taken for Western blot analyses with antibody to the myc epitope. Tubulin was used as a loading control.
doi:10.1371/journal.pgen.1001282.g004

CDC28-VF

It has been suggested that inhibitory phosphorylation of Cdc28, which is antagonized by Cdc55 phosphatase, allows cells to exit from mitosis [22]. Also, previous studies have suggested that this "bypass" could help cells adapt to prolonged mitotic arrest [13,22]. *CDC28-T18V, Y19F* (*CDC28-VF*), a mutant lacking inhibitory phosphorylation sites, delays the exit from mitosis and is hypersensitive to perturbations that arrest cells in mitosis [22,33]. However, these phenotypes result not from lack of inhibitory phosphorylation or increased kinase activity but from reduced activity of the APC/C [33]. Cdc28 is required to induce metaphase-to-anaphase transition by phosphorylation of APC/C components [33,34]. Thus, it is not certain that inhibitory phosphorylation of Cdc28 can be the mechanism of adaptation of the spindle checkpoint.

Our findings suggest that when Cdc28 activates the APC/C by phosphorylation, it simultaneously phosphorylates Bub1 to make it a preferable substrate for degradation, which in turn facilitates deactivation of the spindle checkpoint.

Nocodazole activity

To confirm that nocodazole is not deactivated after incubation for 3 h, yeast medium (YPD) containing 10 μg/mL nocodazole was incubated with yeast cells for 3 h, and fresh cycling yeast cells were incubated in the "used" medium. The FACS profiles showed that the cells were arrested in G2/M after 1.5 h and 2 h

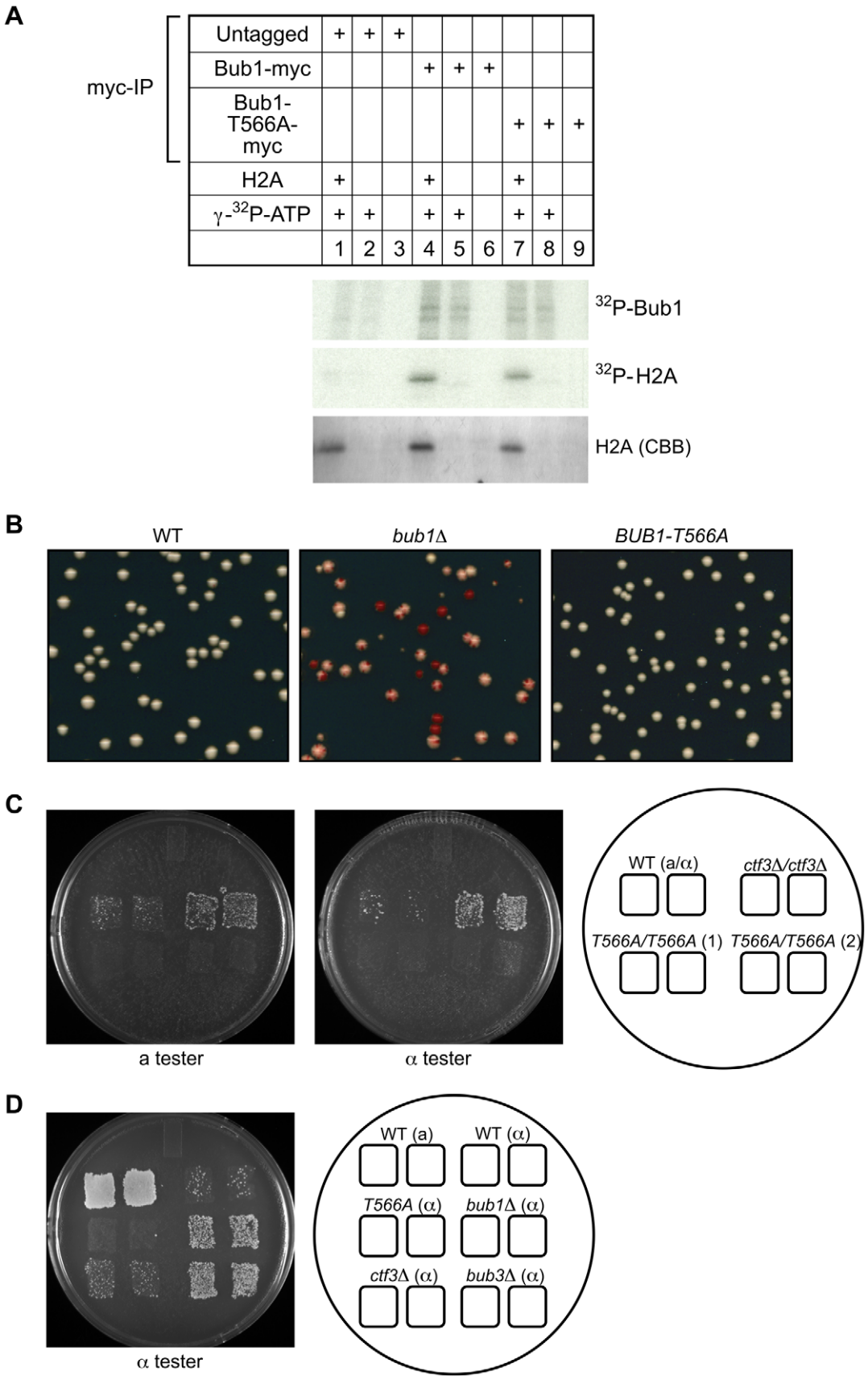

Figure 5. Bub1-T566A mutant has intact kinase activity or kinetochore function. (A) *BUB1-T566A* mutation does not alter kinase activity. Cells expressing Bub1-myc or Bub1-T566A-myc were lysed and immunoprecipitated with antibody to the myc epitope. Immunoprecipitates were

analyzed by performing a kinase assay with 100 μM ATP, 0.2 μCi [gamma-^{32}P]ATP in the presence or absence of human histone H2A recombinant. Coomassie Brilliant Blue staining (CBB) is shown as a loading control. (B) *BUB1-T566A* mutant cells do not display a chromosome missegregation phenotype. The colony color assay was performed as previously described [27,43]. Briefly, wild-type, *bub1Δ* and *BUB1-T566A* mutant cells containing a single *SUP11*-marked chromosome fragment were plated at a density of ~200 colonies per plate on minimal (SD) medium containing a limiting amount of adenine (6 μg/mL) and grown at 30°C. A colony consists of cells containing the chromosome fragment (white) and cells that have lost it (red), resulting in a white-and-red sectored phenotype. (C) *BUB1-T566A* mutant cells do not lose their endogenous chromosome. Diploid strains at *MAT* do not mate because of codominant suppression of haploid-specific cell differentiation pathways. Loss of either the *MATa* or *MATalpha* allele results in mating competence, where mating type is determined by the remaining allele [29,44]. The indicated diploids cells were mated with haploid MATa (17/14) and MAT*alpha* (17/17) tester strains and the mating products were selected. Two independent clones of *BUB1-T566A/BUB1-T566A* mutant cells are shown. (D) *BUB1-T566A* mutant cells do not show elevated a-like faker frequency. Loss of the *MATalpha* locus leads to the default mating type. *MATalpha* cells that lose the *MAT* locus will mate as a-type cells [29,44]. Indicated *MATalpha* strains were mated with the *MATalpha* tester strains (17/17) and mating products were selected.
doi:10.1371/journal.pgen.1001282.g005

incubation, indicating that the nocodazole after incubation for 3 h was still active to arrest cells in G2/M (Figure S11). We also added more nocodazole (the total concentration was 20 μg/mL) at the 2.5 h time point, and we did not see any difference in the numbers of G1 cells at the 5 h time point with or without additional nocodazole (Figure S12). These results indicate that the premature cytokinesis is not due to inactivation of nocodazole.

Adaptation to mitotic arrest induced by the spindle checkpoint

BUB1-T566A mutant cells fail to adapt to the mitotic arrest induced by nocodazole. We found that the T566A protein is stabilized in anaphase, but the T566A mutation does not affect the kinase activity of Bub1. Therefore, the simplest interpretation is that adaptation is induced by Bub1 degradation that is regulated via T566 phosphorylation in anaphase.

If activation of the spindle checkpoint continues, cells eventually die; adaptation to the mitotic arrest gives cells a chance to survive [13,22]. However, adaptation of the spindle checkpoint has a flip side: adapted cells could have an increased chance of aneuploidy due to premature mitotic exit.

Bub1 is functionally highly conserved between yeast and humans. The fission yeast homolog of Bub1 was shown to be phosphorylated by Cdc2 (*Schizosaccharomyces pombe* CDK1) *in vitro*, but none of the sites corresponding to T566 in budding yeast Bub1 [35]. Qi and Yu initially reported that overexpression of human BUB1-KEN box mutant protein that is stable in cells does not cause mitotic arrest or prevent cellular adaptation after prolonged nocodazole treatment [30]. However, the same group has recently found that the KEN boxes of BUB1 are required for the spindle checkpoint in human cells [36]. Also, we found that T566 is conserved in human BUB1 and BUBR1 (Figure S13). Therefore, it is still possible that this adaptation mechanism occurs in humans.

Because aneuploidy may lead to tumorigenesis in humans, either the adaptation might be controlled and balanced precisely or programmed cell death such as apoptosis might occur instead [37,38]. Further studies of this mechanism can improve our understanding of the role of aneuploidy in the development of cancer and drug resistance of cancer cells.

Materials and Methods

Yeast strains, techniques, and media

Media and microbial and genetic techniques were used as described previously [39]. Table S1 presents the genotypes of yeast strains used for this study. Strains that expressed myc- and HA-epitope–tagged proteins were generated by the procedure of Longtine and coworkers [40]. The *BUB1-T566A* mutant was generated as described previously [41] by changing threonine to alanine at position 566. The mutation was verified by sequencing and integrated into the yeast genome. Integrations were amplified by PCR and fragments were sequenced to confirm the change and the strains were generated (see Table S1). To generate *bub1KDΔ* allele, amino acids 710–1021 were truncated by PCR-mediated gene disruption as described previously [40]. Where indicated, cells were arrested in G1 by using the alpha-factor mating pheromone (5 μg/mL; Bio Vectra, Canada). Cells were released from alpha-factor by washing twice in alpha-factor–free media and resuspended in the appropriate medium. Where indicated, the mitotic spindle was disrupted by growing cells in a medium containing nocodazole (Sigma, St. Louis, MO) and benomyl (DuPont, Wilmington, DE) at the indicated final concentration. Expression from the *GAL1* promoter was induced by growing cells in media containing 2% w/v raffinose before transfer to media containing 2% galactose. Expression from the *GAL1* promoter was repressed by adding 2% glucose to the medium. Cells containing the temperature-sensitive *cdc15-2* allele were grown at 23°C and shifted to 37°C to induce anaphase arrest.

Plasmids

Table S2 lists the plasmids used in this study.

Mass spectrometry

The Bub1 phosphorylation site was identified by mass spectrometry performed at the Hartwell Center for Bioinformatics and Biotechnology, St. Jude Children's Research Hospital. A strain with myc epitope–tagged Bub1 was lysed, immunoprecipitated with antibody to the myc epitope, and the immunopurified Bub1 proteins were subjected to SDS-PAGE. The protein in the excised gel band was reduced and alkylated with iodoacetamide and digested with trypsin.

Digests were fractionated by online reverse-phase (C18) ultra-high-pressure liquid chromatography on a nanoAcquity Ultra Performance LC system (Waters Corporation, Milford, MA) using a Waters BEHC18 column (internal diameter of 75 μm, bed length of 10 cm, and particle size of 1.7 μm) and gradient-eluted directly into an LTQ linear ion trap mass spectrometer (Thermo Fisher Scientific, San Jose, CA) using electrospray ionization (ESI). Data dependent scanning was incorporated by acquisition of a full-scan mass spectrum followed by MS/MS on 10 most abundant precursor ions (one micro scan per spectra; precursor m/z ±1.5 Da, 35% collision energy, 30 ms ion activation, 35 s dynamic exclusion, repeat count 2).

Product ions generated by fragmentation along peptide backbone by collision activated dissociation (CAD) (b/y-type ions) were used in an automated database search against yeast BUB1 subset database using Mascot search routine with following residue modifications being allowed: Cysteine (Carbamidomethylation), Methionine (Oxidation) and Serine, Threonine and Tyrosine (Phosphorylation). Phosphopeptide identified from automated search was further validated through manual *de novo* sequencing

of corresponding raw spectrum to assign characteristic fragment ions (b/y-type ions & ions representing loss of phosphoric acid).

Cell synchronization

For G1 arrest, the indicated strains were released from an alpha-factor-induced G1 arrest at 30°C. Samples were taken at the indicated times for FACS analysis.

For G2/M arrest, the indicated strains were tagged with the myc epitope and incubated in the presence of nocodazole at the indicated concentrations; samples were taken for FACS and Western blot analyses.

In *cdc15-2* cells with HA-tagged Bub1 or Bub1-T566A expressed from the *GAL1* promoter (*GAL-BUB1* and *GAL-BUB1-T566A*) were used to test the stability of Bub1 in G1 and in anaphase. The cells were arrested in G1 (alpha-factor at 23°C) and in anaphase (*cdc15-2* at 37°C). The cells were transferred to medium containing galactose (and alpha-factor where appropriate) for 2 h to induce Bub1 expression. Glucose was added to shut-off Bub1 expression; samples were taken at indicated times for Western blot analyses with antibodies to the HA epitope and tubulin protein.

To test the possibility that *BUB1-T566A* mutant cells might have difficulty leaving mitosis, wild-type and *BUB1-T566A* mutant strains were incubated with nocodazole (15 μg/mL) for 90 min at 30°C to induce mitosis and then released from nocodazole arrest; at indicated times, approximately 200 cells were counted to estimate rebudded cells (Figure 4A). All synchronizations were confirmed by FACS analysis.

FACS profile

DNA contents were measured by flow cytometry. The cell culture for each time point was washed with 0.2 M Tris-HCl (pH 7.5) and fixed in 70% ethanol at room temperature for 1 h. Cells were pelleted and resuspended in 200 μl of 0.2 M Tris-HCl (pH 7.5) containing 1 mg/mL RNase A (Sigma, St. Louis, MO). They were then incubated at 37°C for 2 h, centrifuged, resuspended in 200 μg/μL proteinase K (Invitrogen, Carlsbad, CA) for 2 h at 50°C, and stained with 3 μg/mL propidium iodide.

Microscopy

Cells were fixed with 4% paraformaldehyde for 5 min at room temperature. Cells were washed with SK buffer (1 M sorbitol, 50 mM KH_2PO_4 [pH 7.5]) and stained with 1 μg/mL DAPI (4′6′-diamidino-2-phenylindole) for 5 min at room temperature. The cells were washed, sonicated briefly to disrupt clumps, and mounted on glass slides. For time-lapse microscopy, cells were arrested by alpha-factor for 2 h, washed twice with alpha-factor-free media, and spotted onto glass-bottomed culture dish (MatTek, Ashland, MA) containing 2.5 μg/mL nocodazole in a YPD plate. Microscopic images were captured by using a Leica DM IRE2 motorized microscope equipped with an HCX PL FLUOT AR 40x objective lens (Leica, Germany) and images were captured with a ORCA-ER high-resolution digital CCD camera (Hamamatsu Photonics, Japan). All images were analyzed by using Openlab software (Improvision, Lexington, MA). The time-lapse analyses were conducted at 30°C.

Nocodazole and benomyl sensitivity

Sensitivity of the wild-type, *bub1Δ*, and *BUB1-T566A* mutant cells in the presence of nocodazole or benomyl was tested by growing them overnight in YPD at 30°C. Strains were then spotted in 5-fold dilutions from 4×10^7 cells per spot on YPD plates with and without nocodazole or benomyl.

Nocodazole survival assay

The nocodazole survival assay was performed as described previously [42]. Briefly, wild-type, *bub1Δ*, and *BUB1-T566A* mutant cells were incubated with nocodazole (15 μg/mL and 2.5 μg/mL) at the indicated times. Cells were then washed out and approximately 200 cells were plated on a YPD plate. Cell viability was calculated by dividing the number of colonies formed at the 2.5 and 5 h time points by that formed in the absence of nocodazole (0 h) at 30°C.

Sectoring assay

The colony color assay was performed as previously described [27,43]. Briefly, wild-type, *bub1Δ*, and *BUB1-T566A* mutant cells containing a single *SUP11*-marked chromosome fragment were plated at a density of approximately 200 colonies per plate on minimal (SD) medium containing a limiting amount of adenine (6 μg/mL) and grown at 30°C. A colony consists of cells containing the chromosome fragment (white) and cells that have lost it (red), resulting in a white-and-red sectored phenotype.

Diploid bimater and a-Like faker assay

Bimater assay was performed as described previously [29,44]. Diploid *BUB1-T566A/BUB1-T566A* mutants and haploid *BUB1-T566A* mutants were patched onto YPD plates. Diploid cells were replica to both *MATa* and *MATalpha* lawns and haploid cells were replica to *MATalpha* lawns, and mating products were selected.

Kinase assay

The kinase assay was performed as described previously [45]. Briefly, myc-tagged Bub1 and Bub1-T566A cells were immunoprecipitated with a myc epitope antibody and the immunoprecipitate was washed thrice with kinase buffer (50 mM Tris-HCl [pH 7.5], 10 mM $MgCl_2$, and 1% Triton X-100). The volume was reduced to 50 μL, and the solution was incubated with 100 μM ATP, 0.2 μCi [gamma-^{32}P]ATP and substrate (10 μg histone H3 [USBiological, Swampscott, MA]; 1 μg histone H2A human, recombinant [New England BioLabs, MA]; 1 μg histone H1 [Upstate Biotechnology, Lake Placid, NY]; 1 μg BUB1_400-700-MBP and BUB1-T566A_400-700-MBP) at 30°C for 20 min. The reaction was stopped by adding SDS loading buffer, and the protein were then separated by SDS-PAGE, stained with Coomassie Brilliant Blue, and analyzed by autoradiography.

Coimmunoprecipitation assay

Whole-protein extracts for Western blot analysis and immunoprecipitation assays of yeast cell lysates were performed as described previously [46].

Antibodies

Western blot analysis was performed using mouse anti-myc 9E10 purified monoclonal antibody, rat anti-HA purified monoclonal antibody (Roche Applied Science, Indianapolis, IN), and rat YOL1/34 monoclonal anti-tubulin alpha antibody (Serotec, Oxford, UK). The rabbit antibody to phosphorylated T566 of Bub1 was generated by immunizing rabbits (Covance, Denver, PA) with a corresponding KLH-conjugated phosphopeptide (H-TETDVVPIIQpTPKEQIR-OH).

Protein expression

For bacterial expression, BL21-CODONPLUS(DE3)-RIL (Stratagene, La Jolla, CA) cells were transformed with pDEST-HISMBP (Addgene, Cambridge, MA); and protein expression was performed as described previously [47].

Supporting Information

Figure S1 Bub1 kinase domain is not required for T566 phosphorylation. Cells expressing myc-tagged Bub1, Bub1-K733A (a kinase dead mutant), and Bub1-KDΔ (a kinase domain deleted mutant; 1–709 amino acids) were lysed and immunoprecipitated with antibody to the myc epitope. Immunoprecipitates were analyzed with anti-phospho-T566 antibody (α-pT566). The membrane was then stripped and immunoblotted with antibody to the myc epitope (α-myc).
Found at: doi:10.1371/journal.pgen.1001282.s001 (0.15 MB TIF)

Figure S2 Wild-type and *mps1-1* cells with Bub1-myc were grown at 25°C and then shifted to 37°C for 90 min. Cells were lysed and immunoprecipitated with antibody to the myc epitope. Immunoprecipitates were analyzed with anti-phospho-T566 antibody (α-pT566). The membrane was then stripped and immunoblotted with antibody to the myc epitope (α-myc).
Found at: doi:10.1371/journal.pgen.1001282.s002 (0.09 MB TIF)

Figure S3 *BUB1-T566A* is dominant. Wild-type, *BUB1-T566A/BUB1* and *BUB1-T566A/BUB1-T566A* mutant cells were spotted in 5-fold dilutions from 4×10^7cells per spot on a YPD plates with and without benomyl (15 and 20 μg/mL) and incubated at 30°C for 3 days.
Found at: doi:10.1371/journal.pgen.1001282.s003 (0.18 MB TIF)

Figure S4 *BUB1-T566A* mitotic arrest depends on *mad2Δ*. (Upper panel) Wild-type, *bub1Δ*, *BUB1-T566A*, and *BUB1-T566A mad2Δ* cells were incubated with nocodazole (15 μg/mL) at 30°C for 0, 1.5, 2, 2.5, 3, 4 and 5 h; at the indicated times, samples were taken for FACS analysis. (Lower panel) Wild-type, *bub1Δ*, *BUB1-T566A*, and *BUB1-T566A mad2Δ* cells were incubated with nocodazole (15 μg/mL), washed out at the indicated times and approximately 200 cells were plated on a YPD plate. Cell viability was calculated by dividing the number of colonies formed at the 2.5 and 5 h time points by that formed in the absence of nocodazole (0 h) at 30°C.
Found at: doi:10.1371/journal.pgen.1001282.s004 (0.27 MB TIF)

Figure S5 Wild-type and *BUB1-T566A* cells were incubated with nocodazole (2.5 μg/mL) and washed out at the indicated times. Approximately 200 cells were plated on a YPD plate. Cell viability was calculated by dividing the number of colonies formed at the 2, 4, 6, 8 and 12 h time points by that formed in the absence of nocodazole (0 h) at 30°C.
Found at: doi:10.1371/journal.pgen.1001282.s005 (0.07 MB TIF)

Figure S6 Quantification of the results shown in Figure 4C, lower panel. Data represent the relative protein concentration estimated by measuring the intensity of Bub1-HA bands relative to the intensity of tubulin bands.
Found at: doi:10.1371/journal.pgen.1001282.s006 (0.08 MB TIF)

Figure S7 Quantification of the results shown in Figure 4D. Data represent the relative protein amounts estimated by measuring the intensity of Bub1-Myc bands relative to the intensity of tubulin bands.
Found at: doi:10.1371/journal.pgen.1001282.s007 (0.08 MB TIF)

Figure S8 Cells expressing Bub1-myc or Bub1-T566A-myc were lysed and immunoprecipitated with antibody to the myc epitope. Immunoprecipitates were analyzed by performing kinase assay with 100 μM ATP, 0.2 μCi [gamma-^{32}P] ATP in the presence or absence of histone H3. Coomassie Brilliant Blue staining (CBB) is shown as a loading control.
Found at: doi:10.1371/journal.pgen.1001282.s008 (0.16 MB TIF)

Figure S9 Strains with Bub1-myc cells were arrested by alpha-factor and released from G1. Cells were taken for co-immunoprecipitation analyses. The cells were lysed and immunoprecipitated with antibody to the myc epitope. Immunoprecipitates were analyzed with anti-phospho-T566 antibody (α-pT566). The membrane was then stripped and immunoblotted with antibody to the myc epitope (α-myc). DNA content was measured by FACS analysis.
Found at: doi:10.1371/journal.pgen.1001282.s009 (0.29 MB TIF)

Figure S10 Asynchronous Bub1-myc cells and Bub1-myc cells synchronized in G1 (alpha-factor), S phase (Hydroxyurea) and G2/M (Nocodazole) were lysed and immunoprecipitated with antibody to the myc epitope. Immunoprecipitates were analyzed with anti-phospho-T566 antibody (α-pT566). The membrane was then stripped and immunoblotted with antibody to the myc epitope (α-myc). DNA content was measured by FACS analysis.
Found at: doi:10.1371/journal.pgen.1001282.s010 (0.19 MB TIF)

Figure S11 Wild-type and *BUB1-T566A* cells were incubated with nocodazole (10 μg/mL) at 30°C. At the 3 h time point, the half of the cells were centrifuged, and the supernatant was transferred to fresh cycling cells and incubated for additional 1.5 h and 2 h. At the indicated times, samples were taken for FACS analysis.
Found at: doi:10.1371/journal.pgen.1001282.s011 (0.08 MB TIF)

Figure S12 Wild-type and *BUB1-T566A* cells were incubated with nocodazole (10 μg/mL) at 30°C. At the 2.5 h time point, additional nocodazole (the total concentration was 20 μg/mL) was added to the half of the cells. At the indicated times, samples were taken to count the G1 cells.
Found at: doi:10.1371/journal.pgen.1001282.s012 (0.07 MB TIF)

Figure S13 Alignment of the amino acid sequences of Human BUB1 and BUBR1 and budding yeast BUB1 is shown.
Found at: doi:10.1371/journal.pgen.1001282.s013 (0.07 MB TIF)

Table S1 Strains used in this study.
Found at: doi:10.1371/journal.pgen.1001282.s014 (0.11 MB DOC)

Table S2 Plasmids used in this study.
Found at: doi:10.1371/journal.pgen.1001282.s015 (0.05 MB DOC)

Video S1 Wild-type cells were arrested by alpha-factor and released from G1 onto plates containing 2.5 μg/mL nocodazole at 30°C. Time-lapse images were taken at the indicated times. The time-lapse experiment was performed 4 times, and all showed essentially the same results.
Found at: doi:10.1371/journal.pgen.1001282.s016 (7.27 MB ZIP)

Video S2 *BUB1-T566A* mutant cells were arrested by alpha-factor and released from G1 onto plates containing 2.5 μg/mL nocodazole at 30°C. Time-lapse images were taken at the indicated times. The time-lapse experiment was performed 4 times, and all showed essentially the same results.
Found at: doi:10.1371/journal.pgen.1001282.s017 (6.78 MB ZIP)

Acknowledgments

We thank S. Biggins, V. Measday, R. Kitagawa, P. K. Bansal, and A. D. Rudner for their helpful comments; members of the Katsumi and Risa Kitagawa laboratories for stimulating conversation and advice; P. Hieter and A. W. Murray for their generous gifts of reagents; and Vani Shanker for editing this manuscript.

Author Contributions

Conceived and designed the experiments: GHG CAS KK. Performed the experiments: GHG AM RA. Analyzed the data: GHG AM CAS KK. Contributed reagents/materials/analysis tools: RA. Wrote the paper: GHG AM KK.

References

1. Inoue S, Salmon ED (1995) Force generation by microtubule assembly/disassembly in mitosis and related movements. Mol Biol Cell 6: 1619–1640.
2. Michaelis C, Ciosk R, Nasmyth K (1997) Cohesins: chromosomal proteins that prevent premature separation of sister chromatids. Cell 91: 35–45.
3. Rieder CL, Schultz A, Cole R, Sluder G (1994) Anaphase onset in vertebrate somatic cells is controlled by a checkpoint that monitors sister kinetochore attachment to the spindle. J Cell Biol 127: 1301–1310.
4. Schaar BT, Chan GK, Maddox P, Salmon ED, Yen TJ (1997) CENP-E function at kinetochores is essential for chromosome alignment. J Cell Biol 139: 1373–1382.
5. Skibbens RV, Skeen VP, Salmon ED (1993) Directional instability of kinetochore motility during chromosome congression and segregation in mitotic newt lung cells: a push-pull mechanism. J Cell Biol 122: 859–875.
6. Skibbens RV, Rieder CL, Salmon ED (1995) Kinetochore motility after severing between sister centromeres using laser microsurgery: evidence that kinetochore directional instability and position is regulated by tension. J Cell Sci 108(Pt 7): 2537–2548.
7. Wood KW, Sakowicz R, Goldstein LS, Cleveland DW (1997) CENP-E is a plus end-directed kinetochore motor required for metaphase chromosome alignment. Cell 91: 357–366.
8. Guacci V, Hogan E, Koshland D (1994) Chromosome condensation and sister chromatid pairing in budding yeast. J Cell Biol 125: 517–530.
9. Ciosk R, Zachariae W, Michaelis C, Shevchenko A, Mann M, et al. (1998) An ESP1/PDS1 complex regulates loss of sister chromatid cohesion at the metaphase to anaphase transition in yeast. Cell 93: 1067–1076.
10. Uhlmann F, Lottspeich F, Nasmyth K (1999) Sister-chromatid separation at anaphase onset is promoted by cleavage of the cohesin subunit Scc1. Nature 400: 37–42.
11. Uhlmann F, Wernic D, Poupart MA, Koonin EV, Nasmyth K (2000) Cleavage of cohesin by the CD clan protease separin triggers anaphase in yeast. Cell 103: 375–386.
12. Cohen-Fix O, Peters JM, Kirschner MW, Koshland D (1996) Anaphase initiation in Saccharomyces cerevisiae is controlled by the APC-dependent degradation of the anaphase inhibitor Pds1p. Genes Dev 10: 3081–3093.
13. Rudner AD, Murray AW (1996) The spindle assembly checkpoint. Curr Opin Cell Biol 8: 773–780.
14. Li R, Murray AW (1991) Feedback control of mitosis in budding yeast. Cell 66: 519–531.
15. Hoyt MA, Totis L, Roberts BT (1991) S. cerevisiae genes required for cell cycle arrest in response to loss of microtubule function. Cell 66: 507–517.
16. Wells WA, Murray AW (1996) Aberrantly segregating centromeres activate the spindle assembly checkpoint in budding yeast. J Cell Biol 133: 75–84.
17. Palframan WJ, Meehl JB, Jaspersen SL, Winey M, Murray AW (2006) Anaphase inactivation of the spindle checkpoint. Science 313: 680–684.
18. Vanoosthuyse V, Hardwick KG (2009) A novel protein phosphatase 1-dependent spindle checkpoint silencing mechanism. Curr Biol 19: 1176–1181.
19. Pinsky BA, Nelson CR, Biggins S (2009) Protein phosphatase 1 regulates exit from the spindle checkpoint in budding yeast. Curr Biol 19: 1182–1187.
20. Kung AL, Sherwood SW, Schimke RT (1990) Cell line-specific differences in the control of cell cycle progression in the absence of mitosis. Proc Natl Acad Sci U S A 87: 9553–9557.
21. Rieder CL, Palazzo RE (1992) Colcemid and the mitotic cycle. J Cell Sci 102(Pt 3): 387–392.
22. Minshull J, Straight A, Rudner AD, Dernburg AF, Belmont A, et al. (1996) Protein phosphatase 2A regulates MPF activity and sister chromatid cohesion in budding yeast. Curr Biol 6: 1609–1620.
23. Ubersax JA, Woodbury EL, Quang PN, Paraz M, Blethrow JD, et al. (2003) Targets of the cyclin-dependent kinase Cdk1. Nature 425: 859–864.
24. Farr KA, Hoyt MA (1998) Bub1p kinase activates the Saccharomyces cerevisiae spindle assembly checkpoint. Mol Cell Biol 18: 2738–2747.
25. De Brabander MJ, Van de Veire RM, Aerts FE, Borgers M, Janssen PA (1976) The effects of methyl (5-(2-thienylcarbonyl)-1H-benzimidazol-2-yl) carbamate, (R 17934; NSC 238159), a new synthetic antitumoral drug interfering with microtubules, on mammalian cells cultured in vitro. Cancer Res 36: 905–916.
26. Fernius J, Hardwick KG (2007) Bub1 kinase targets Sgo1 to ensure efficient chromosome biorientation in budding yeast mitosis. PLoS Genet 3: e213. doi:10.1371/journal.pgen.0030213.
27. Koshland D, Hieter P (1987) Visual assay for chromosome ploidy. Methods Enzymol 155: 351–372.
28. Shero JH, Koval M, Spencer F, Palmer RE, Hieter P, et al. (1991) Analysis of chromosome segregation in Saccharomyces cerevisiae. Methods Enzymol 194: 749–773.
29. Montpetit B, Hazbun TR, Fields S, Hieter P (2006) Sumoylation of the budding yeast kinetochore protein Ndc10 is required for Ndc10 spindle localization and regulation of anaphase spindle elongation. J Cell Biol 174: 653–663.
30. Qi W, Yu H (2007) KEN-box-dependent degradation of the Bub1 spindle checkpoint kinase by the anaphase-promoting complex/cyclosome. J Biol Chem 282: 3672–3679.
31. Taylor SS, Hussein D, Wang Y, Elderkin S, Morrow CJ (2001) Kinetochore localisation and phosphorylation of the mitotic checkpoint components Bub1 and BubR1 are differentially regulated by spindle events in human cells. J Cell Sci 114: 4385–4395.
32. Brady DM, Hardwick KG (2000) Complex formation between Mad1p, Bub1p and Bub3p is crucial for spindle checkpoint function. Curr Biol 10: 675–678.
33. Rudner AD, Hardwick KG, Murray AW (2000) Cdc28 activates exit from mitosis in budding yeast. J Cell Biol 149: 1361–1376.
34. Rudner AD, Murray AW (2000) Phosphorylation by Cdc28 activates the Cdc20-dependent activity of the anaphase-promoting complex. J Cell Biol 149: 1377–1390.
35. Yamaguchi S, Decottignies A, Nurse P (2003) Function of Cdc2p-dependent Bub1p phosphorylation and Bub1p kinase activity in the mitotic and meiotic spindle checkpoint. EMBO J 22: 1075–1087.
36. Kang J, Yang M, Li B, Qi W, Zhang C, et al. (2008) Structure and substrate recruitment of the human spindle checkpoint kinase Bub1. Mol Cell 32: 394–405.
37. Kitagawa K, Niikura Y (2008) Caspase-independent mitotic death (CIMD). Cell Cycle 7: 1001–1005.
38. Niikura Y, Dixit A, Scott R, Perkins G, Kitagawa K (2007) BUB1 mediation of caspase-independent mitotic death determines cell fate. J Cell Biol 178: 283–296.
39. Rose MD, Winston F, Hieter P (1990) Methods in Yeast Genetics: Cold Spring Harbor Laboratory Press, Cold Spring Harbor, NY.
40. Longtine MS, McKenzie A, 3rd, Demarini DJ, Shah NG, Wach A, et al. (1998) Additional modules for versatile and economical PCR-based gene deletion and modification in Saccharomyces cerevisiae. Yeast 14: 953–961.
41. Kitagawa K, Abdulle R (2002) In vivo site-directed mutagenesis of yeast plasmids using a three-fragment homologous recombination system. Biotechniques 33: 288, 290, 292 passim.
42. Burton JL, Solomon MJ (2007) Mad3p, a pseudosubstrate inhibitor of APCCdc20 in the spindle assembly checkpoint. Genes Dev 21: 655–667.
43. Gerring SL, Spencer F, Hieter P (1990) The CHL 1 (CTF 1) gene product of Saccharomyces cerevisiae is important for chromosome transmission and normal cell cycle progression in G2/M. EMBO J 9: 4347–4358.
44. Yuen KW, Warren CD, Chen O, Kwok T, Hieter P, et al. (2007) Systematic genome instability screens in yeast and their potential relevance to cancer. Proc Natl Acad Sci U S A 104: 3925–3930.
45. Kitagawa K, Abdulle R, Bansal PK, Cagney G, Fields S, et al. (2003) Requirement of Skp1-Bub1 interaction for kinetochore-mediated activation of the spindle checkpoint. Mol Cell 11: 1201–1213.
46. Kitagawa K, Skowyra D, Elledge SJ, Harper JW, Hieter P (1999) SGT1 encodes an essential component of the yeast kinetochore assembly pathway and a novel subunit of the SCF ubiquitin ligase complex. Mol Cell 4: 21–33.
47. Bansal PK, Abdulle R, Kitagawa K (2004) Sgt1 associates with Hsp90: an initial step of assembly of the core kinetochore complex. Mol Cell Biol 24: 8069–8079.